Journal of Materials and Environmental Sciences
ISSN : 2028-2508
CODEN : JMESCN

J. Mater. Environ. Sci., 2018, Volume 9, Issue 8, Page 2254-2262

http://www.jmaterenvironsci.com

Hirshfeld Surface Analysis and DFT calculations of 1-phenyl-N-(benzomethyl)-N-({1-[(2-benzo-4-methyl-4,5-dihydro-1,3-oxazol-4-yl)methyl]-1H-1,2,3-triazol-4-yl}methyl)methanamine

S. Boukhssas[1], Y. Aouine[2], H. Faraj[2], A. Alami[2]*, A. El Hallaoui[2], N. Tijani[3], K. Yamni[3], H. Zouihri[3], D. Mrani[4] and M. Lachkar[5]

[1]*Doctoral Training "Bioactive Molecules, Health and Biotechnology", Center of Doctoral Studies "Sciences and Technology", LCO, Faculty of Sciences Dhar Mahraz – Sidi Mohammed Ben Abdellah University, Morocco.*
[2]*Organic Chemistry Laboratory (LCO), Faculty of Sciences Dhar Mahraz – Sidi Mohammed Ben Abdellah University,Morocco.*
[3]*Laboratory of Materials Chemistry and Biotechnology of Natural Products, Moulay Ismail University, Faculty of Sciences, Meknes, Morocco*
[4]*Faculty of Sciences and Technology, Moulay Ismail University, Po. Box 509, Errachidia, Morocco.*
[5]*Engineering Laboratory of Organometallic and Molecular Materials, Faculty of Sciences Dhar Mahraz – Sidi Mohammed Ben Abdellah University,Morocco.*

Received 26 Oct 2017,
Revised 23 Apr 2018,
Accepted 06 May 2018

Keywords
- ✓ 1,2,3-Triazoles,
- ✓ Azide–alkyne cycloaddition,
- ✓ Hirshfeld surface,
- ✓ DFT calculations,

A. Alami
anouar.alami@usmba.ac.ma
+21235733171

Abstract

X-ray analysis results of 1-phenyl-N-(benzomethyl)-N-({1-[(2-benzo-4-methyl-4,5-dihydro-1,3-oxazol-4-yl)methyl]-1H-1,2,3-triazol-4-yl}methyl)methanamine are compared with the optimized structure computed by using B3LYP method with 6-31G basis set as provided with Gaussian 03 software. The calculated results showed that optimized geometry can well reproduce the crystal structure parameters. The Hirshfeld surfaces and consequently the fingerprint analysis have been performed to study the nature of interactions and their quantitative contributions towards the crystal packing. The electrostatic potential has been mapped over the Hirshfeld surface to explore the electrostatic complementarity, which exists in the crystal packing. It is found that the weak interactions, such as C—H…Cg, Cg—Cg are significant contributors in the stabilization of the crystal packing in addition to the presence of strong C–H…N hydrogen bonds.

1. Introduction

The study of the nature of intermolecular interactions and its control is extremely important in the area of crystal engineering in order to design a new material of desirable properties [1,2] and also for crystal structure prediction of a given set of molecules [3-5]. The formation of crystal or molecular aggregation of a compound depends on a complex phenomenon known as molecular recognition which is achieved through hydrogen bonds or other weak non covalent interactions [6,7]. In this regards, nature of strong hydrogen bond e.g. N–H…O/N, O– H…O/N are now well understood and appeared most reliable in molecular recognition processes and hence found to direct the crystal packing [8,9]. The recent focus in supramolecular chemistry is shifted towards understanding the nature and capabilities of weak interactions such as C–H…O/N,C–H…π, π…π, etc. in the formation of supramolecular assemblies and finally its correlation with the material properties [10]. Since the nature of weak intermolecular interactions and its influences in the crystal packing appeared as unpredictable in nature, therefore careful but systematic studies of its nature has been become an important prerequisite in the

area of crystal engineering. This can be preferably carried out by either systematically changing the position of functional groups (positional isomers) of interest in the desired compound [11,12] or systematic replacement of the functional group with others [13]. To get a better understanding of the contribution of intermolecular interactions to the crystal packing, it is important to get a quantitative evaluation of these interactions [14,15]. The theoretical calculation of the lattice energy of a crystal provides a better idea about the nature of crystal packing which corresponds to the experimentally calculated sublimation energy of the compound [16-18]. The Density Functional Theory (DFT) is a computational method that derives properties of the molecule based on a determination of the electron density of the molecule, It is based on empirical partitioning of the interaction energy or cohesive energy into their coulombic, polarization, dispersion and repulsion contributions and provides important insights towards an understanding of the crystal packing.

In this present study, the 1-phenyl-N-(benzomethyl)-N-({1-[(2-benzo-4-methyl-4,5-dihydro-1,3-oxazol-4-yl)methyl]-1H-1,2,3-triazol-4-yl}methyl)methanamine [19,20] has been synthesized and the presence of strong H-bonds, weak intermolecular interactions and stacking interactions have been quantified. The chemical groups which constitute this molecule are the substituted triazole ring and the oxazole ring. In view of the above-mentioned applications, a systematic exploration and quantification of the molecular geometry and intermolecular interactions is expected to contribute towards an understanding of the forces which favour formation of the crystal in this class of molecules. The geometrical parameters, fundamental frequencies of the new 1,2,3-Triazole derivative in the ground state have been calculated by using the DFT (B3LYP) and HF methods with 6-31G (p,d) basis set. This calculation is valuable for providing insight into molecular parameters and the vibration spectrum. The aim of this work was to explore the molecular structural parameters that govern the chemical behaviour, and to compare predictions made from theory with experimental observations.

2. Material and Methods

2.1. Theoretical calculations

The geometry of the title compound was optimized using the DFT (density functional theory) method with B3LYP (Becke three-parameter LeeYang-Parr) and PBE hybrid density functional theories, HF (Hartree-Fock) method and MP2 (Second-order Møller–Plesset theory), all with the 3-21G basis set. It has been reported that the employment of this basis set (3-21G) along with several electronic structure methods, predicts chemical shifts with acceptable accuracy, and the obtained results present a good correlation between the experimental and theoretical values. Calculations were performed by taking the crystal structure coordinates as an initial geometryand carried out with Gaussian 03 software package.All geometric parameters were visualized with GaussView 5.0 software. Calculated geometries of the title compound were compared with experimental values reported from crystallographic data. This test allowed the selection of the best method for geometry optimization.

The energy gap between HOMO and LUMO was calculated. According to the frontier molecular orbital theory, HOMO and LUMO are the most important factors that affect the bioactivity. HOMO has the priority to provide electrons, while LUMO can accept electrons first. Thus, the study on the frontier orbital energy can provide useful information about the biological mechanism.

2.2. Hirshfeld surface analysis

Although experimental electron densities can be determined, they offer incomplete insight into molecular packing because of the absence of knowledge of the surface at which one molecule ‘ends’ and another ‘begins’. Hirshfeld surfaces overcome this problem by replacing each atom with its spherically averaged theoretical electron density counterpart. The origin of each contribution to the total electron density is thus known. The surface generated by those points at which the calculated electron density from the chosen molecule equals that from the surrounding molecules defines the Hirshfeld surface. Inside this surface, the electron density is dominated by the electron density belonging to the chosen molecule. Bonding interactions are ignored but this should not be important in external regions of space.

Hirshfeld surfaces [21] and the associated 2D-fingerprint plots [22] were generated using CrystalExplorer 3.0. [23] Hirshfeld surfaces mapped with different properties e.g. de, dnorm, shape index, curvedness, has proven to be a useful visualization tool for the analysis of intermolecular interactions and the crystal packing behaviour of molecules [24]. Figures 1 and 2 lists the Hirshfeld surfaces of all the molecule in the present study mapped with the above-mentioned properties.

Electrostatic potentials mapped on Hirshfeld surfaces provide direct insight into intermolecular interactions in crystals. The molecular electrostatic potential (MEP) map displays electrostatic potential regions of the molecules using simple colour coding. The MEP is used to determine the electrophilic and nucleophilic attacks during the reactions as well as hydrogen bonding interactions. The map is obtained at HF/3-21G level of theory. Moreover, blue and red colours indicate the positive and negative potentials, respectively. The negative electrostatic potential is usually associated with the lone pair of electronegative atoms.

The 2D-fingerprint plot provides decomposition of Hirshfeld surfaces into contribution of different intermolecular interactions present in crystal structure. Hence both Hirshfeld surfaces and fingerprint plots facilitates the comparison of intermolecular interactions in building different supramolecular motifs in the crystal structure. The electrostatic potentials were also mapped on the Hirshfeld surfaces to allows the visual study of electrostaticcomplementarities in the crystal packing analysis.

3. Results and discussion

3.1. X-Ray Crystal Structures

The X-ray structure analysis of title compound, $C_{28}H_{29}N_5O$, indicates that all the bond lengths in the title compound fall in normal ranges. All C—C (with a mean distance 1.4175A), C—N (with a mean distance 1.4135 A) and C—O (with a mean distance 1.4028 A) bond lengths are comparable to those in related compounds. The dihedral angles between the three benzene rings and the oxazole and triazole groups are: 83.50 (7)°, 68.37 (7)°, 11.74 (7)°, 17.46 (6)°, 86.69 (7)° and 77.16 (7)°, respectively. There are some C—H…N hydrogen bonds in the lattice of the title compound that make it form a one-dimensional chain.The crystal packing is stabilized into three-dimensional network by additional C—H···N H-bonds, C—H···π and π···π interactions.

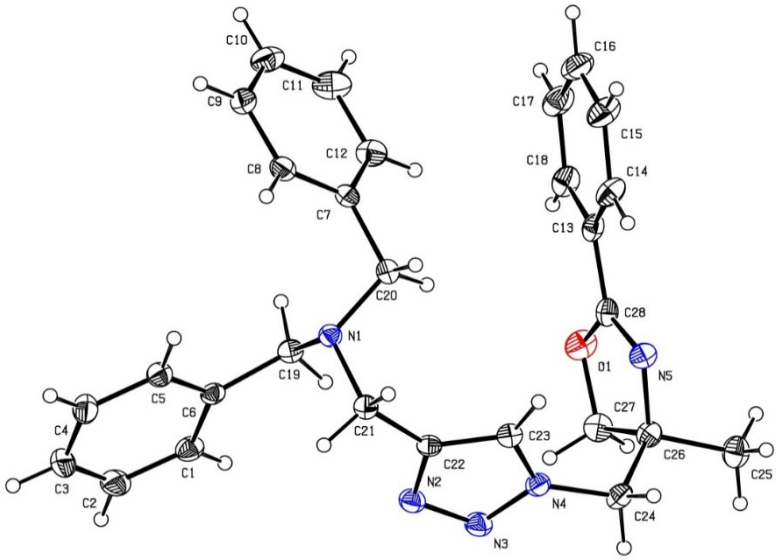

Figure 1:Molecular view of the title compound showing the atom-labeling scheme. Displacement ellipsoids are drawn at the 50% probability level. H atoms are represented as small spheres of arbitrary radii.

3.2. Hirshfeld Surface Analysis

The intermolecular interactions of the title compound are quantified using Hirshfeld surface analysis. This approach is used to estimate the intermolecular contacts, which are shown in Fig. 2. These inter-contacts are

highlighted by conventional mapping of dnorm on molecular Hirshfeld surfaces are shown in Fig. 1. The red spots over the surface indicate the intercontacts involved in the hydrogen bonds.

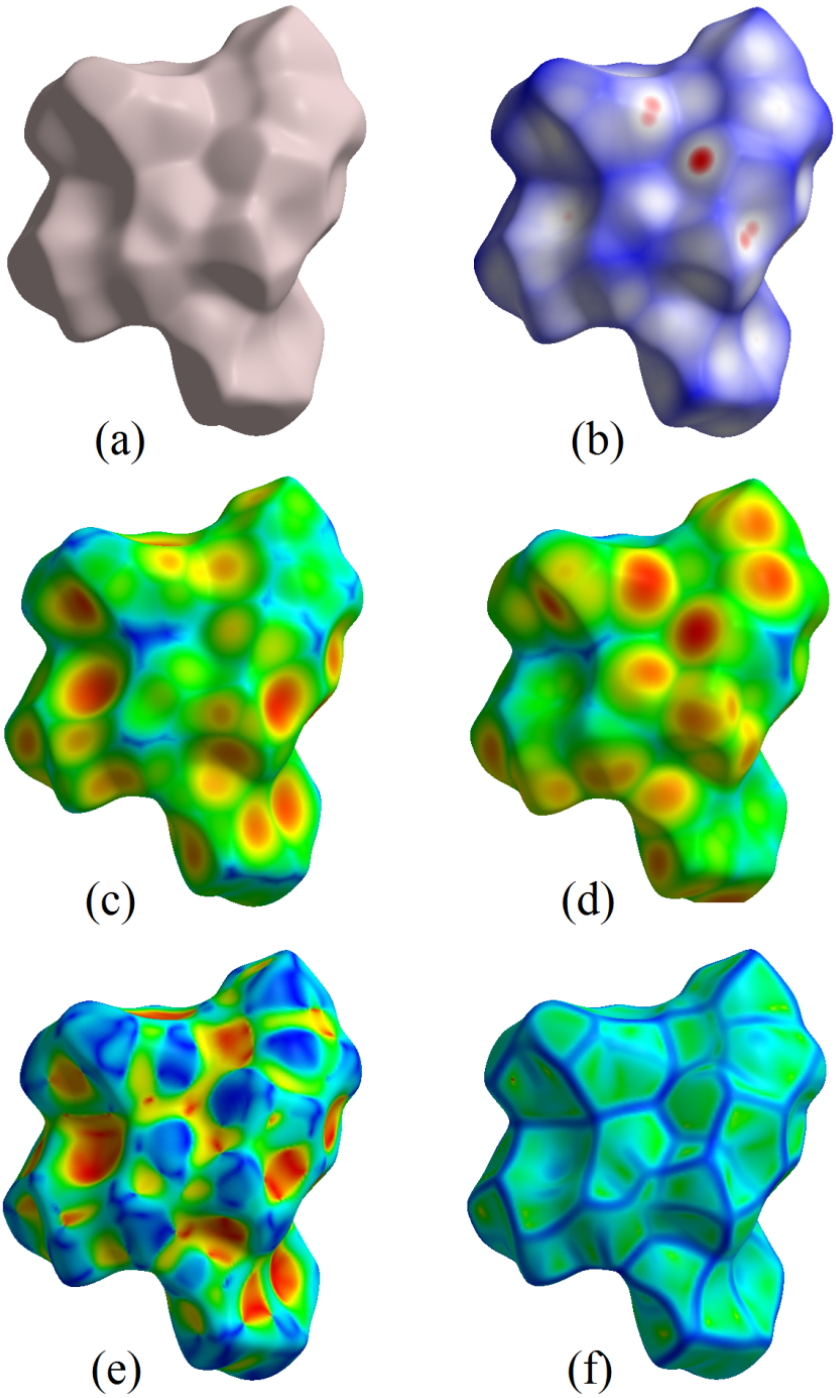

Figure 2:Hirshfeld surfaces of the molecule of $C_{28}H_{29}N_5O$: (b) dnorm, (c) de, (d) di, (c) Shape index and (d) Curvedness.

Further, intercontacts were plotted with fingerprint plots (Fig. 3). H...H intercontacts, (Fig.3(c)) shows large surfaces, whereas the O...H plot (reciprocal interactions included) (Fig. 3(f)) shows the presence of O...H contact with the two characteristic wings. The intercontacts N...H (Fig. 3(e)) showing two narrow pointed wings provide evidence for C-H...N classical hydrogen bonds, the full fingerprint appears as a gray shadow (Fig. 3(a)). The chart indicates that the contribution of inter-contacts to the Hirshfeld surfaces, H...H (61.6%), C...H (24.3%), N...H (10.5%) and O...H (3.5%), the quantitative results of the Hirshfeld surface analysis are presented in Fig. 4.

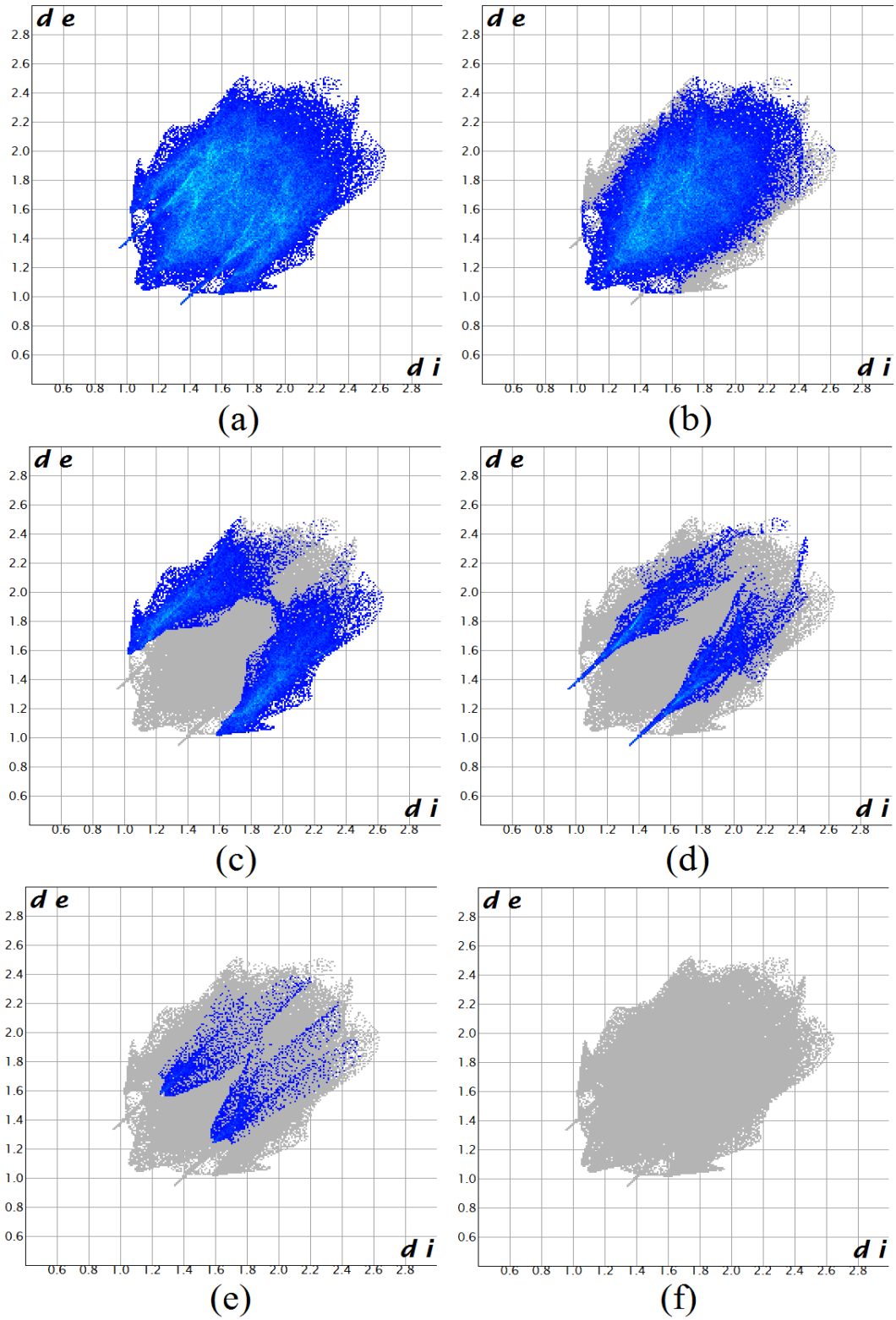

Figure 3:Fingerprint of the title compound, (b) H...H, (c) C...H, (c) N...H and (d) O...H. The outline of the full fin-gerprint is shown in gray. di is the closest internal distance from a given point on the Hirshfeld surface and de is the closest external contacts.

The electrostatic potential is mapped on Hirshfeld surface using STO-3G basis set at the Hartree-Fock theory over the range of ± 0.025 au clearly shows the positions of close intermolecular contacts in the compound (Fig. 5b). The positive electrostatic potential (blue region) over the surface indicates hydrogen donor potential, whereas the hydrogen bond acceptors are represented by negative electrostatic potential (red region) [25].

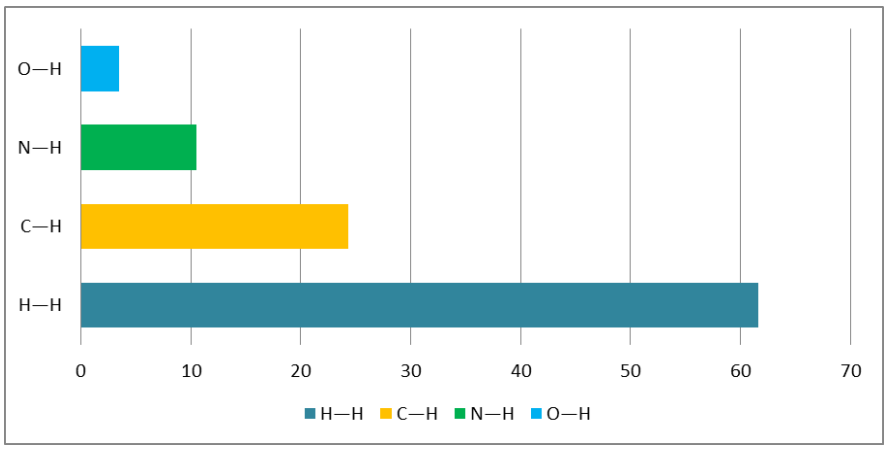

Figure 4: Percentage contribution of individual intermolecular interactions to the Hirshfeld surfaces of compound.

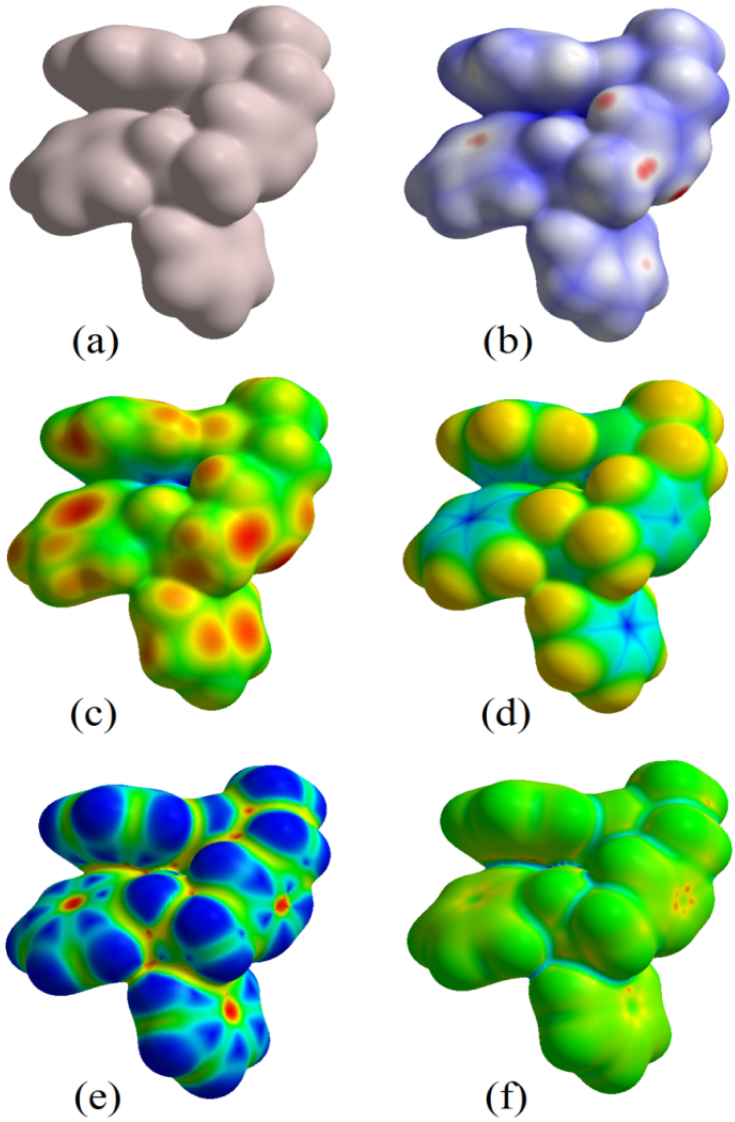

Figure 5:Electrostatic Potential (PE) mapped on Hirshfeld surface of the molecule of $C_{28}H_{29}N_5O$: (b) dnorm, (c) de, (d) di, (e) Shape index and (f) Curvedness.

3.3. Optimized geometry

The DFT (PBEPBE//3-21G, B3LYP//3-21G), Hartree-Fock (HF//3-21G) and MP2//3-21G levels calculations were carried out to predict the geometry of the title molecule compound. The actual and optimized bond lengths and angles, which were obtained by X-ray crystallographic study as well as by geometry optimizations are reported in the Fig.6.

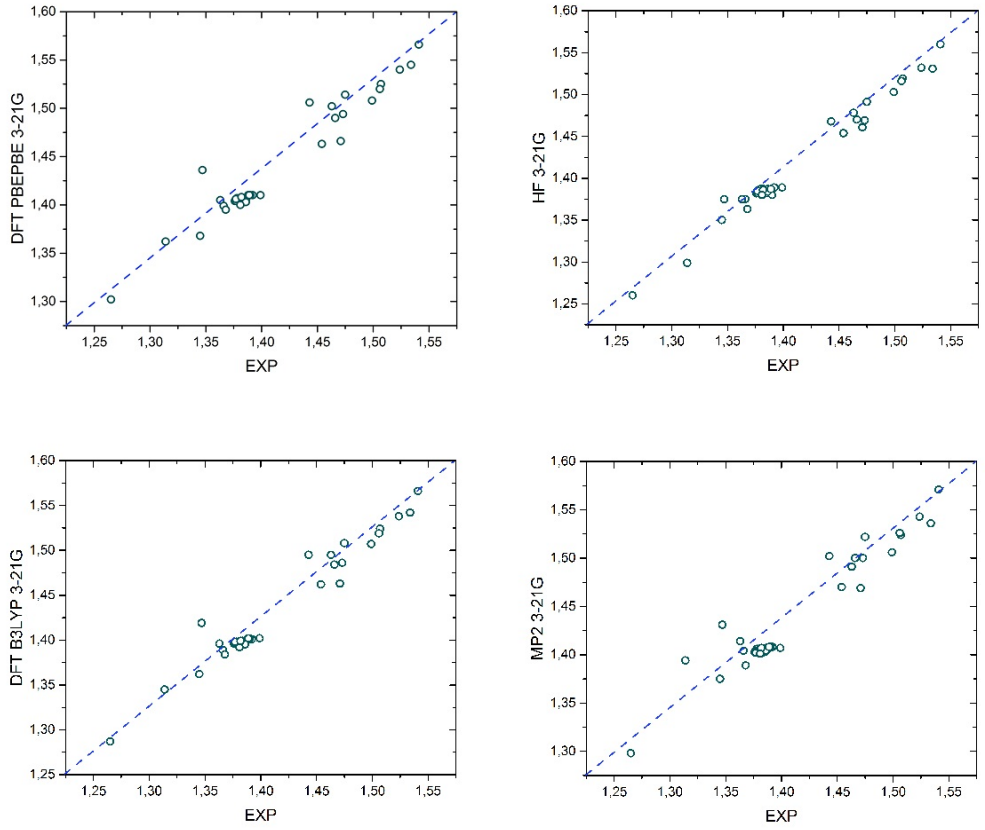

Figure 6: Graphic correlation between the experimental and the theoretical values of bond distances and bond angles obtained by PBEPBE//3-21G, HF//3-21G, B3LYP//3-21G and MP2//3-21G.

Considering the data from graphics above, some main structural parameters differ slightly between the X-ray and the theoretical structure. From all HF, MP2 and DFT methods with 3-21G calculations basis, the HF//3-21G was the most accurate method used for the geometry optimization of the title molecule. It should be noticed that slight differences in bond parameters are attributed to the fact that the experimental results belong to solid phase while theoretical calculations belong to gaseous phase.

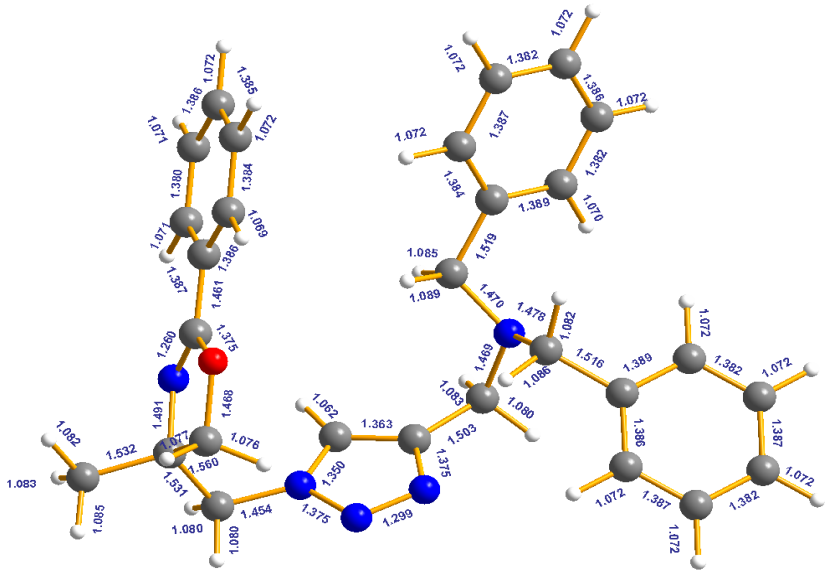

Figure 7: The HF//3-21G optimized geometry of the title compound; values of bond lenths (Å) are given.

The highest occupied molecular orbital (HOMO) energies, the lowest unoccupied molecular orbital (LUMO) energies, and the energy gap for mentioned molecule in above have calculated. The calculated HOMO–LUMO gap of the title molecule is 4.105eV by DFT//B3LYP, 2,295 eV by DFT//PBEPBE, 8,340 eV by HF//3-21G and 5.98 eV by MP2//3-21G. The molecular HOMO/LUMO orbital pictures are depicted in Fig.8. Generally, the total energy is relatively low but the energy gap of HOMO-LUMO is small, suggesting that the stability of the compound is poor [26].

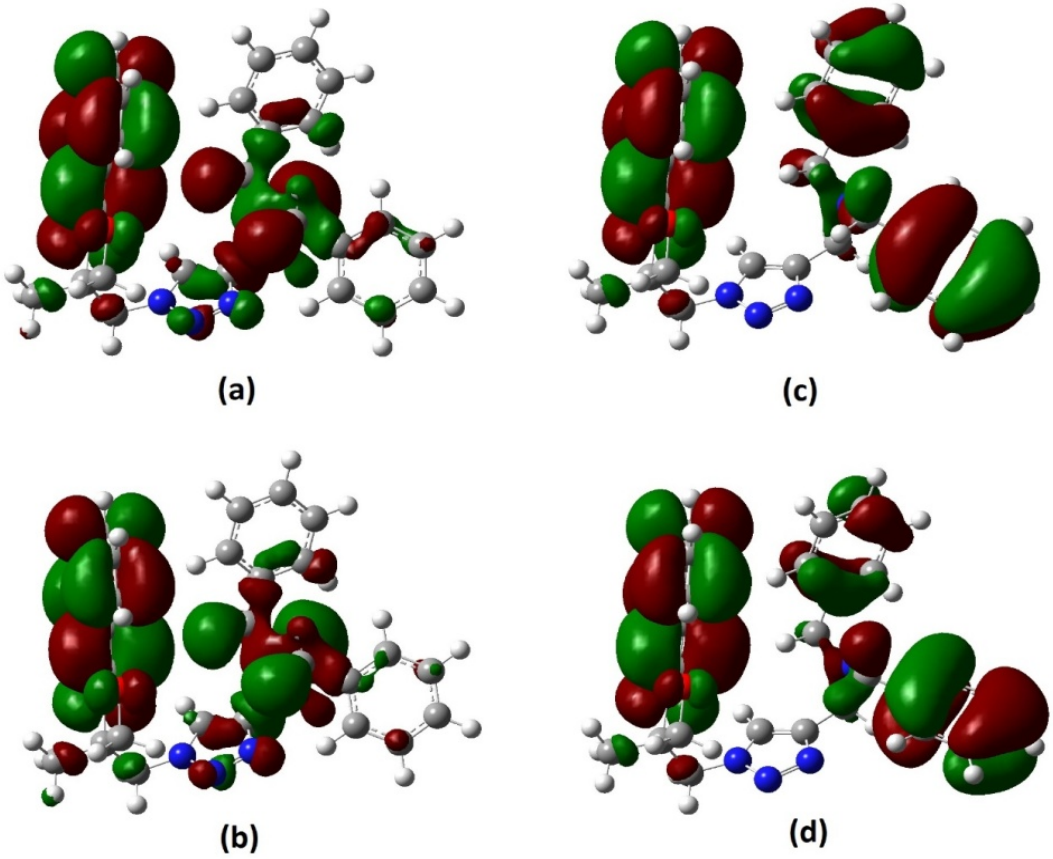

Figure 8: Molecular orbital HOMO-LUMO diagram of the title compound: (a) DFT//B3LYP(EHOMO = -0.04712 a.u, ELUMO = -0.19799 a.u), (b) DFT//PBEPBE (EHOMO = -0.07537 a.u, ELUMO = -0.15974 a.u), (c) HF//3-21G (EHOMO = -0.09169 a.u, ELUMO = -0.31379 a.u) et (d) MP2//3-21G (EHOMO = -0.08263 a.u, ELUMO = -0.30646 a.u).

Conclusion

To summarize, In this work we have reported the Hirshfeld surfaces analyses of 1-phenyl-N-(benzomethyl)-N-({1-[(2-benzo-4-methyl-4,5-dihydro-1,3-oxazol-4-yl)methyl]-1H-1,2,3-triazol-4-yl}methyl)methanamine. The formation of the molecular compound was further characterized and confirmed by NMR spectroscopy analysis. The 3D Hirshfeld surface analysis and 2D fingerprint maps analysis revealed that H…H and C…H interactions are more dominant in the title compound.The analysis of ESP mapped on the Hirshfeld surface complements the importance of electrostatic complementarity in the crystal packing.

For a detailed molecular structure description some quantum-chemical calculations were performed with several HF, MP2 and DFT methods. The comparison of the theoretical results with experimental X-ray diffraction data for similar compounds, showed that, from all the tested methods, the best performance for geometrical parameters was for HF (in combination with a large basis set 3-21G).

Considering all HF, MP2 and DFT methods with 3-21G calculations basis, the HF//3-21G was the most accurate method used for the geometry optimization of the title molecule. All calculations were done using the Gaussian 03 software package. Theoretical calculations can be used to predict and confirm the structure of the new substituted 1,2,3-triazole with good correlation with the experimental data.

References

1. A. Nangia and G. R. Desiraju. in Design of Organic Solids. [éd.] Springer-Verlag. Berlin : ed. E. Weber, (1998).
2. C. B. Aakeroy, N. R. Champness and C. Janiak, , *Cryst. Eng. Comm*., 12 (2010) 22.
3. V. R. Vangala, B. R. Bhogala, A. Dey, G. R. Desiraju, C. K. Broder, P. S. Smith, R. Mondal, J. A. K. Howard and C. C. Wilson, , *J. Am. Chem. Soc*., 125 (2003) 14495.
4. M. Tremayne, L. Grice, J. C. Pyatt, C. C. Seaton, B. M. Kariuki, H. H. Y. Tsui, S. L. Price and J. C. Cherryman, *J. Am. Chem. Soc*., 126 (2003) 7071.
5. A. Dey, M. T. Kirchner, V. R. Vangala, G. R. Desiraju, R. Mondal and J. A. K. Howard,. *J. Am. Chem. Soc*., 127 (2005) 10545.
6. G. A. Jeffrey. An Introduction to Hydrogen Bonding. [éd.] Oxford University Press. Oxford,: s.n., (1997).
7. G. R. Desiraju and T. Steiner. The Weak Hydrogen Bond in Structural Chemistry and Biology. [éd.] Oxford University Press. Oxford,: s.n., (1999).
8. G. R. Desiraju, *Angew. Chem., Int. Ed*., 50 (2011) 52.
9. E. Arunan, G. R. Desiraju, R. A. Klein, J. Sadlej, S. Scheiner, I. Alkorta, D. C. Clary, R. H. Crabtree, J. J. Dannenberg, P. Hobza, H. G. Kjaergaard, A. C. Legon, B. Mennucci and D. J. Nesbitt, *Pure Appl. Chem*., 83 (2011) 1619.
10. C. M. Reddy, G. R. Krishna and S. Ghose, *Cryst. Eng. Comm*., 12 (2010) 2296.
11. D. Chopra and T. N. Guru Row, *Cryst. Eng. Comm*., 10 (2008) 54.
12. P. Panini and D. Chopra, *Cryst. Eng. Comm*., 14 (2012) 1972.
13. D. Chopra, V. Thiruvenkatam, S. G. manjunath and T. N. Guru Row, *Cryst. Growth Des*., 7 (2007) 868.
14. G. Kaur, P. Panini, D. Chopra and A. R. Choudhury, *Cryst. Growth Des*., 12 (2012) 5096.
15. P. Panini and D. Chopra, *Cryst. Eng. Comm*., 15 (2013) 3711.
16. B. Cavalleri, C. M. Zicovich-Wilson, L. Valenzano and P. Ugliengo, *Cryst. Eng. Comm*., 10 (2008) 405.
17. J. D. Dunitz and A. Gavezzotti, *Chem. Soc. Rev*., 38 (2009) 2622.
18. L. Maschio, B. Civalleri, P. Ugliengo and A. Gavezzotti, *J. Phys. Chem.* A, 115 (2011) 11179.
19. Y. Aouine, A. El Hallaoui, A.Alami, *Molbank*, M819 (2014).
20. S. Boukhssas, Y. Aouine, H. Faraj,A. Alami, A.El Hallaoui and H. Zouihri, , *IUCrData*, 2 (2017), x170860.
21. M. A. Spackman and D. Jayatilaka, 2009, Cryst. Eng. Comm., Vol. 11, p. 19.
22. J. J. McKinnon, D. Jayatilaka and M. A. Spackman, *Chem. Commun*., (2007) 3814.
23. S. K. Wolff, D. J. Grimwood, J. J. McKinnon, M. J. Turner, D. Jayatilaka and M. A. Spackman, CrystalExplorer (Version 3.0), . [prod.] University of Western Australia. (2012).
24. J. J. McKinnon, M. A. Spackman and A. S. Mitchell, 2004,*Acta Crystallogr., Sect*. B: *Struct. Sci*., 60 (2004) 627.
25. M. A. Spackman, J. J.McKinnon, D. Jayatilaka, *Cryst. Eng. Comm*., 10(2008) 377.
26. M. J. Frisch, G. W. Trucks, H. B. Schlegel, G. E. Scuseria, M. A. Robb, J. R. Cheeseman, J. A. Montgomery Jr., T. Vreven, K. N. Kudin, J. C. Burant, J. M. Millam, S. S. Iyengar, J. Tomasi, V. Barone, B. Mennucci, M. Cossi, G. Scalmani, N. Rega, G. A. Petersson, H. Nakatsuji, M. Hada, M. Ehara, K. Toyota, R. Fukuda, J. Hasegawa, M. Ishida, T. Nakajima, Y. Honda, O. Kitao, H. Nakai, M. Klene, X. Li, J. E. Knox, H. P. Hratchian, J. B. Cross, C. Adamo, J. Jaramillo, R. Gomperts, R. E. Stratmann, O. Yazyev, A. J. Austin, R. Cammi, C. Pomelli, J. W. Ochterski, P. Y. Ayala, K. Morokuma, G. A. Voth, P. Salvador, J. J. Dannenberg, V. G. Zakrzewski, S. Dapprich, A. D. Daniels, M. C. Strain, O. Farkas, D. K. Malick, A. D. Rabuck, K. Raghavachari, J. B. Foresman, J. V. Ortiz, Q. Cui, A. G. Baboul, S. Clifford, J. Cioslowski, B. B. Stefanov, G. Liu, A. Liashenko, P. Piskorz, I. Komaromi, R. L. Martin, D. J. Fox, T. Keith, M. A. Al-Laham, C. Y. Peng, A. Nanayakkara, M. Challacombe, P. M. W. Gill, B. Johnson, W. Chen, M. W. Wong, C. Gonzalez and J. A. Pople, Gaussian 03, Revision E.01 (Gaussian, Wallingford, CT, 2004).

(2018) ; http://www.jmaterenvironsci.com